The Journal of Neuroscience, November 15, 1998, *18*(22):9192–9203

Na,K-ATPase Subunit β1 *knock-in* Prevents Lethality of β2 Deficiency in Mice

Philipp Weber,[1] **Udo Bartsch,**[1] **Melitta Schachner,**[1,2] **and Dirk Montag**[1,3]

[1]*Department of Neurobiology, Swiss Federal Institute of Technology, CH-8093 Zürich, Switzerland,* [2]*Zentrum für Molekulare Neurobiologie, Universität Hamburg, D-20246 Hamburg, Germany and* [3]*Research Group Neurogenetics, Leibniz Institute for Neurobiology, D-39118 Magdeburg, Germany*

The β2 subunit of the Na,K-ATPase displays functional properties of both an integral constituent of an ion pump and an adhesion and neurite outgrowth-promoting molecule *in vitro*. To investigate whether the β1 subunit of the Na,K-ATPase can functionally substitute for the β2 isoform *in vivo*, we have generated β2/β1 *knock-in* mice by homologous recombination in embryonic stem cells. In β2/β1 *knock-in* mice, expression of β2 was abolished, whereas β1 mRNA expression from the mutated gene amounted to ~15% of the normal expression of β2 in the adult mouse brain and prevented the juvenile lethality observed for β2 null mutant mice. In contrast to β2 null mutant mice, the overall morphological structure of all analyzed brain regions was normal. By immunohistochemical analysis, β1 expression was detected in photoreceptor cells in the retina of *knock-in* mice at an age when expression of β1 and β2, respectively, is downregulated and persisting in the wild-type mice. Morphological analysis by light and electron microscopy revealed a progressive degeneration of photoreceptor cells. Apoptotic death of photoreceptor cells determined quantitatively by terminal deoxynucleotidyl transferase-mediated dUTP nick end labeling analysis increased in β2/β1 *knock-in* mice with age. These observations suggest that the β1 subunit of the Na,K-ATPase can substitute sufficiently, at least in certain cell types, for the role of the β2 subunit as a component of a functional Na,K-ATPase, but they do not allow us to determine the possible role of the β2 subunit as an adhesion molecule *in vivo*.

Key words: Na,K-ATPase; knock-in*; retinitis pigmentosa; photoreceptor cells; adhesion molecule on glia; AMOG; mouse; β subunit; ionic homeostasis*

The Na,K-ATPase is an ubiquitously expressed ion pump located in the plasma membrane. The pump maintains the flux of sodium and potassium ions across membranes and thus regulates, by directly influencing ion gradients, cellular activities such as cell volume and size, action potentials, and secondary active transport systems. The functional Na,K-ATPase is a heterodimeric ion pump which consists of a α subunit and a β subunit. Three α subunits (α1, α2, and α3) and three β subunits (β1, β2, and β3) have been identified (Mercer et al., 1986; Shull et al., 1986; Hara et al., 1987; Herrera et al., 1987; Gloor, 1989; Malik et al., 1996). The α subunit comprises the catalytic and transport activities of the Na,K-ATPase (Jørgensen and Andersen, 1988; Skou, 1990; Blanco et al., 1994). The functional role of the β subunit is less well understood, but it appears to be involved in the structural maturation, correct routing of the functional heterodimeric Na,K-ATPase to the plasma membrane, and localization of the α subunit in the plasma membrane (Geering et al., 1989, 1996; McDonough et al., 1990; Geering, 1991). Combinations of different α subunits (α1, α2, and α3) with β subunits (β1, β2, β3) by recombinant expression in *Xenopus* oocytes show that different α and β subunits can associate with each other to form functionally active pumps (Horisberger et al., 1991; Schmalzing et al., 1991, 1992, 1997; Jaisser et al., 1992; Munzer et al., 1994; Blanco et al., 1995a,b; Therien et al., 1996).

The subunits of the Na,K-ATPase show distinct expression patterns. The α1 subunit is expressed in all tissues. α2 is expressed mainly in skeletal muscle and also in brain and heart, and α3 is expressed only in brain and heart (Emanuel et al., 1987; Orlowski and Lingrel, 1988). Expression of the β1 subunit is detected in most neural cells, being predominantly located in neurons and astrocytes (Lecuona et al., 1996; Peng et al., 1997). During the second postnatal week, expression of the β1 subunit by glial cells and photoreceptor cells in the optic nerve and the retina, respectively, is downregulated (Lecuona et al., 1996). The β2 subunit of the Na,K-ATPase is predominantly expressed by glial cells in the CNS and additionally by distinct neuronal cell types, including, for instance, granule cells in the cerebellar cortex and photoreceptor cells in the retina (Magyar et al., 1994). Expression of β2 is first detectable in the brain at late embryonic stages, increases during the first 2 postnatal weeks, and reaches highest levels in the adult (Pagliusi et al., 1990; Lecuona et al., 1996), whereas it is hardly detectable outside the CNS (Antonicek et al., 1987; Antonicek and Schachner, 1988; Gloor et al., 1990; Pagliusi et al., 1990). β3 subunit expression has been detected in human placenta and various rat tissues, including skeletal muscle and lung of 7-d-old animals and the developing and

Received July 22, 1998; revised Aug. 27, 1998; accepted Sept. 1, 1998.

We thank Dr. J. P. Magyar for providing genomic clones pBlueKS+/AMOG, pGem2/MmATPb1, pGem2/MmATPb2, and pUC19-G7SH2.1, and Dr. S. Gloor for providing clone pBSKS+AMOG2. We are grateful to Dr. H. Blüthmann and Y. Lang for providing feeder cells, Dr. J. P. Julien and his coworkers for generation of chimeric mice, Kathrin Mannigel for animal care, and Christiane Born for technical assistance. We thank Drs. K. Geering, S. Gloor, and K. J. Sweadner for critically reading this manuscript.

Correspondence should be addressed to Dr. Dirk Montag, Leibniz Institute for Neurobiology, Research Group Neurogenetics, Brenneckestrasse 6, D-39118 Magdeburg, Germany.

Dr. Weber's present address: Institut de Génétique et de Biologie Moleculaire et Cellulaire, Centre National de la Recherche Scientifique/Institut National de la Santé et de la Recherche Médicale/Université Louis Pasteur, Collège de France, BP163, F-67404 Illkirch-Cedex, France.

Dr. Bartsch's present address: Zentrum für Moleculare Neurobiologie, Universität Hamburg, D-20246 Hamburg, Germany.

 0270-6474/98/189192-12$05.00/0

adult brain (Malik et al., 1996; Arystarkhova and Sweadner, 1997).

The β2 subunit of the Na,K-ATPase was originally identified as an adhesion molecule on glia (AMOG) mediating adhesion between neurons and astrocytes (Antonicek et al., 1987; Antonicek and Schachner, 1988). Sequence analysis of AMOG identified it as a homolog of the β1 subunit of the Na,K-ATPase (Gloor et al., 1990). Here, we refer to AMOG as the β2 subunit of the Na,K-ATPase. The β2 subunit, but not the β1 subunit of the Na,K-ATPase, promotes neurite outgrowth *in vitro* (Müller-Husmann et al., 1993). A monoclonal antibody to β2 that blocks adhesion increases Na,K-ATPase activity of cultured astrocytes (Gloor et al., 1990). The dual function of the β2 subunit in cell recognition and ion transport has been hypothesized to couple cell recognition with regulation of the ionic milieu (Gloor et al., 1990). Mice deficient in β2 exhibit lack of motor coordination at 15 d of age and subsequent tremor and paralysis of extremities, and they die at 17–18 d after birth (Magyar et al., 1994). Morphological analysis of the CNS of 17-d-old β2-deficient mice revealed enlarged ventricles, swollen astrocytic end feet in the brain stem, thalamus, and spinal cord, and apoptotic photoreceptor cell death in the retina during the second postnatal week (Magyar et al., 1994; Molthagen et al., 1996).

Analysis of the phenotype of β2-deficient mice led to the interpretation that the morphological abnormalities could be caused by the absence of pump activity or the absence of adhesion molecule function or both. In the hope of distinguishing between these possibilities, we generated β2/β1 *knock-in* mutant mice via homologous recombination in embryonic stem cells. In these animals, the β1 subunit cDNA is placed into the β2 gene, yielding the replacement of β2 expression by β1 expression under the regulatory elements of the β2 gene. Here we show that in contrast to β2-deficient animals, β2/β1 *knock-in* mutants have a normal life span. Moreover, swollen and enlarged astrocytic end feet were not detectable in the brain stem of *knock-in* mutants. Degeneration of photoreceptor cells was reduced in β2/β1 *knock-in* mutants when compared with β2 null mutants, but it was significantly increased when compared with wild-type animals.

MATERIALS AND METHODS

β2/β1 targeting construct. The targeting construct consisted of a 1 kb 5′ region of the mouse β2 gene and the mouse cDNA coding for the β1 subunit of the Na,K-ATPase inserted in frame into the unique XmnI site in exon I of the β2 gene, followed by a 4.7 kb 3′ region of the β2 gene containing exons II to VII (Magyar et al., 1994) (see Fig. 1*A–C*). By use of the conserved XmnI site in the β2 genomic sequence and in the β1 cDNA sequence, a fusion between the sequence coding for 18 amino acids of the N-terminal part of β2 and the cDNA sequence coding for amino acids 14 to 304 of the β1 isoform (Gloor, 1989) (see Fig. 1*D*) was obtained. The herpes simplex virus (HSV) thymidine kinase gene (*tk*) at the 3′ end of the construct allowed for selection against random integration (Mansour et al., 1988). For positive selection, the neomycin resistance gene driven by the PGK promoter (Soriano et al., 1991) and flanked by loxP sites and polyadenylation sites (loxpAPGK*neo*pAlox) was inserted 3′ to the β1 cDNA sequence, resulting in the targeting construct designated β2/β1loxpA*neo*lox*tk* (see Fig. 1*B*).

Cell culture. The embryonic stem cell line E14.1 (Hooper et al., 1987) was cultured on irradiated primary mouse embryonic fibroblasts (MEF). Embryonic stem cells (2×10^7) were transfected by electroporation (Bio-Rad Gene Pulser; 230V, 500 μF) with 20 μg of *Sal*I linearized targeting construct, cultured on irradiated MEF^{neoR} feeder cells (gift of Dr. H. Blüthmann, F. Hofmann-LaRoche, Basel, Switzerland), and selected with 0.2 μM 1-(2-deoxy, 2-fluoro-β-D-arabinofuranosyl)-5-iodouracil (FIAU) (Bristol-Myers, New York, NY) and 300 μg/ml G418 (Life Technologies-BRL, Rockville, MD) for 3 and 6 d, respectively. Single colonies were expanded, and aliquots of clones were frozen as described (Chan and Evans, 1991) or cultured in medium containing 60% buffalo rat liver cell-conditioned medium without feeder cells for DNA isolation.

Screening of recombinant clones and Southern blot analysis. Embryonic stem cells were lysed and DNA was isolated as described (Ramirez-Solis et al., 1992). DNA of individual embryonic stem cell clones was digested with *Bam*HI and analyzed by Southern blotting as described (Montag et al., 1994) using the probe 5′EXT (416 bp *Sty*I-*Sna*BI fragment of the β2 gene 5′ of the construct) (see Fig. 1*C*). The probe was labeled to 10^8 cpm/μg according to Feinberg and Vogelstein (1983). Genomic DNA from positive embryonic stem cells was further characterized after restriction with appropriate enzymes by Southern blot analysis as described above using probe 3′INT (1690 bp fragment from XmnI exon I to *Eco*RV intron I) (see Fig. 1*C*).

Blastocyst injection and mating of mice. Blastocyst injections were performed by Dr. J. P. Julien and his coworkers (McGill University, Montreal, Canada) on a commercial basis. Male chimeras were mated with C57BL/6J females. Heterozygous offspring were crossed to obtain homozygous mice. The genotype of mice was determined by Southern blot analysis of DNA isolated from tail biopsies.

RNA preparation and Northern blot analysis. Total RNA from brains of 5-week-old wild-type ($\beta2/\beta1^{+/+}$), heterozygous ($\beta2/\beta1^{+/ki}$), and homozygous ($\beta2/\beta1^{ki/ki}$) β2/β1 *knock-in* mice was isolated using the RNeasy Kit (QIAGEN, Santa Clarita, CA). RNA was electrophoresed in a 1.5% agarose gel containing 7% formaldehyde and transferred onto Hybond-N membranes (Amersham, Uppsala, Sweden). Hybridization was performed with the following random-primed probes (cDNA probes labeled to 10^8 cpm/μg): 1079 bp *Eco*RI fragment of construct β2/β1loxpA*neo*lox*tk* coding for the β1 cDNA (probe β1), 686 bp *Pst*I-*Eco*RV fragment of pBSKS+AMOG2 encoding exons II to VII of β2 (probe β2), and 625 bp *Apa*I-*Sac*II fragment of BlueKS+/AMOG (probe β2–5′UT), representing 556 bp of 5′ untranslated and 75 bp translated sequence of the β2 gene. Relative mRNA expression levels were estimated by visual comparison of band intensities.

Antibodies. Polyclonal antibody to the mouse β2 subunit, monoclonal antibodies 426 and BSP/3 to the mouse β2 and β1 subunits, respectively, and polyclonal antibodies to mouse L1 have been described (Gorvel et al., 1984; Rathjen and Schachner, 1984; Antonicek et al., 1987; Schmalzing et al., 1991). For indirect immunofluorescence, polyclonal and monoclonal antibodies were visualized by fluorescein isothiocyanate (FITC)-conjugated antibodies to rat or rabbit IgG (diluted 1:100) (Dako, Hamburg, Germany).

Protein analysis of brain extracts. For analysis of proteins, retinae of 17-d-old or brains of 5-week-old wild-type ($\beta2/\beta1^{+/+}$) and β2/β1 *knock-in* mice ($\beta2/\beta1^{ki/ki}$) were homogenized in buffer H (1 mM $NaHCO_3$, 0.2 mM $CaCl_2$, 0.2 mM $MgCl_2$, 1 mM spermidine, pH 7.9) complemented with protease inhibitors (10 μg/ml soybean trypsin inhibitor, 10 μg/ml turkey egg-white trypsin inhibitor, 1 mM phenylmethylsulfonyl fluoride, 0.5 mM iodoacetamide). The homogenate was centrifuged at 4°C and 30,000 × *g* for 30 min. The pellet was solubilized for 2 hr at 4°C in buffer S (20 mM Tris, 1 mM EDTA, 1 mM EGTA, 0.15 M NaCl, 0.5% Triton X-100, pH 7.2) complemented with protease inhibitors as detailed above. The solubilized fraction was centrifuged at 4°C and 100,000 × *g* for 45 min. The protein concentrations of supernatants of crude membrane fractions were determined using the BCA-assay (Pierce, Rockford, IL). After addition of 2× loading buffer and heat denaturation, samples were analyzed under reducing (L1) or nonreducing conditions (polyclonal anti-β2 antibody, BSP/3) by SDS-PAGE (Laemmli, 1970) and Western blotting (Towbin et al., 1979). Primary antibodies were visualized using horse radish peroxidase-coupled antibodies to rat or rabbit IgG (diluted 1:10,000) (Dianova, Hamburg, Germany) and detection by enhanced chemiluminescence (ECL kit; Amersham). Relative protein expression levels were estimated by visual comparison of band intensities.

For deglycosylation of β1 in tissue homogenates of retinae, membrane fractions (10 μg of protein) from 17-d-old wild-type ($\beta2/\beta1^{+/+}$) and β2/β1 *knock-in* mice ($\beta2/\beta1^{ki/ki}$) were incubated with *N*-glycosidase F (PNGase F) and/or *O*-glycosidase as described (Holm et al., 1996). The proteins were resolved and subjected to immunoblot analysis as described above.

Light and electron microscopy. For light and electron microscopy, mice were deeply anesthetized and perfused through the left ventricle with 4% paraformaldehyde and 2% glutaraldehyde in 0.1 M phosphate buffer, pH 7.4. Tissue was removed and post-fixed in the same fixative for 2 hr at room temperature. Vibratome sections of eyes dissected through central regions of the retina and of brains, 200–500 μm in thickness, were

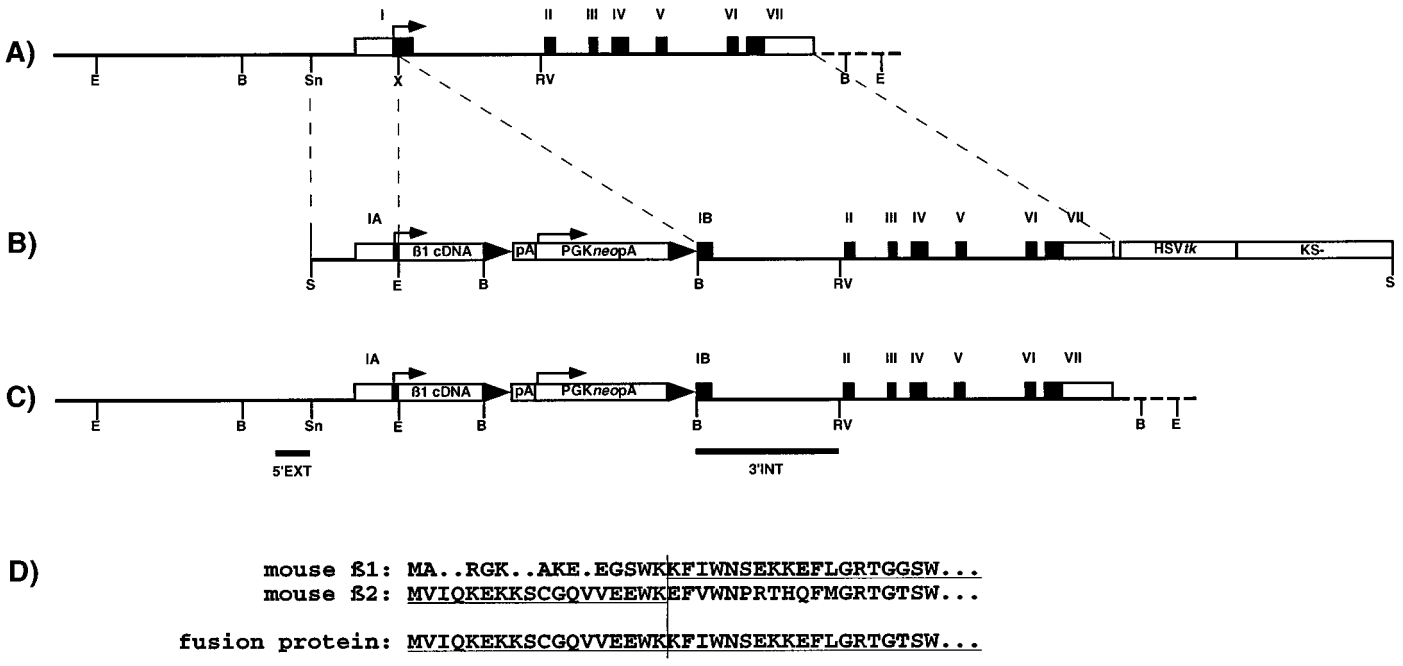

Figure 1. β2 gene, β2/β1 *knock-in* targeting construct, and structure of the β2/β1 *knock-in* gene. *A*, Restriction map of the mouse β2 gene. Translated and nontranslated exons are represented by *closed* and *open boxes*, respectively, and are numbered with *Roman numerals*. *E, B, Sn, X*, and *RV* represent cleavage sites for *Eco*RI, *Bam*HI, *Sna*BI, *Xho*I, and *Eco*RV (not all sites indicated), respectively. *Arrow* indicates the translation initiation codon. *B*, Restriction map of the β2/β1 *knock-in* targeting construct β2/β1loxpA*neo*lox*tk*, containing 1.0 and 4.7 kb of homologous sequences on the 5′ and 3′ site flanking the β1cDNAloxpA*neo*pAlox insertion and thus interrupting β2 gene in exon I. LoxP sites are indicated by *triangles*, the β1 cDNA, the PGK*neo*bpA cassette, the HSV*tk* cassette, and the Bluescript (KS-) vector are indicated by *open boxes*. *S* represents cleavage sites for *Sal*I. *C*, Expected and observed structure of the β2/β1 *knock-in* gene after homologous recombination and localization of probes. *Horizontal bars* indicate the localization of hybridization probes 5′EXT and 3′INT. *D*, Alignment of N-terminal amino acid sequences of β1 and β2 subunits and the β2/β1 fusion protein. Residues of the β1 and β2 subunit contributing to the fusion protein are *underlined*. The *vertical bar* indicates the fusion site.

incubated in 2% OsO_4 for 2 hr, dehydrated in an ascending series of methanol, and embedded in Epon resin as described (Bartsch et al., 1989; Montag et al., 1994). For light microscopy, 3-μm-thick sections were stained with Toluidine blue and examined with a Zeiss Axiophot microscope. For electron microscopy, ultrathin sections were counterstained with lead citrate and examined with a Zeiss EM 10C electron microscope.

Immunohistochemistry. Indirect immunofluorescence on sections of fresh-frozen retinae was performed as described including the negative controls with secondary antibodies only (Bartsch et al., 1989; Wintergerst et al., 1993).

Visualization of apoptotic cell death. To visualize degenerating cells in the retina, fragmented DNA of apoptotic cells was detected using the terminal deoxynucleotidyl transferase-mediated dUTP nick end labeling (TUNEL) technique (Gavrieli et al., 1992). Briefly, cryosections through central regions of the retinae from 17-d-old, 4-month-old, and 9-month-old wild-type ($\beta2/\beta1^{+/+}$) and β2/β1 *knock-in* mice ($\beta2/\beta1^{ki/ki}$) were mounted onto silan-coated coverslips and processed as described (Molthagen et al., 1996). Sections were finally mounted onto slides and analyzed with a fluorescence microscope (Axiophot, Zeiss). Labeled cells in the outer nuclear layer were counted at a final magnification of 200×. Subsequently, sections were counterstained with Toluidine blue, and the area of the outer nuclear layers was determined using an image analysis system (Neurolucida V2.1i, MicroBrightFields). At least three animals were analyzed for each genotype and age. Statistical analysis of data was performed using ANOVA and the Fischer's protected least significant difference test (Fischer's PLSD).

RESULTS

Generation of β2/β1 *knock-in* mice

After electroporation of the linearized targeting vector into strain 129Ola-derived embryonic stem cells and double selection with FIAU and G418, 1 in 20 clones carried the expected mutation as determined by Southern blot analysis with the external probe 5′EXT (Fig. 1). In addition to the wild-type band of 8.4 kb, the appearance of a 2.9 kb band was detected because of the presence of a new *Bam*HI site introduced by insertion of the β1 cDNA sequence into exon I of the β2 gene (Fig. 2*A*). Further analysis with the 3′ internal probe 3′INT confirmed the pattern expected after homologous recombination.

Highly chimeric mice were obtained after injection of targeted embryonic stem cells into blastocysts. Chimeric males showed germline transmission of the integrated β1 cDNA sequence as confirmed by Southern blot analysis. Crossing of heterozygous offspring yielded homozygous β2/β1 *knock-in* mice with Mendelian frequencies. Southern blot analysis of these mice with probes 5′EXT and 3′INT showed the pattern expected for a single integration by homologous recombination (Fig. 2*A*). Neither heterozygous nor homozygous β2/β1 *knock-in* mice showed any obviously abnormal behavioral phenotype. In contrast to β2-deficient mice, β2/β1 *knock-in* mice had a life span not different from wild-type mice (data not shown).

Total RNA from brains of 5-week-old wild-type, heterozygous, and homozygous β2/β1 *knock-in* mice was subjected to Northern blot analysis to determine whether the mutated β2 gene was transcribed (Fig. 2*B*). After hybridization with probe β2, no signal was detectable with RNA from β2/β1 *knock-in* mice. In contrast, β2 mRNA of ~3.0 kb was easily detectable in wild-type and heterozygous animals (Fig. 2*B*). After hybridization with probe β1, similar amounts of β1 mRNA in the range of 1.5 to 2.5 kb were detectable in wild-type, heterozygous, and homozygous mice (Fig. 2*B*). To distinguish between endogenous and *knock-in*-derived β1 mRNA, the Northern blot was hybridized with

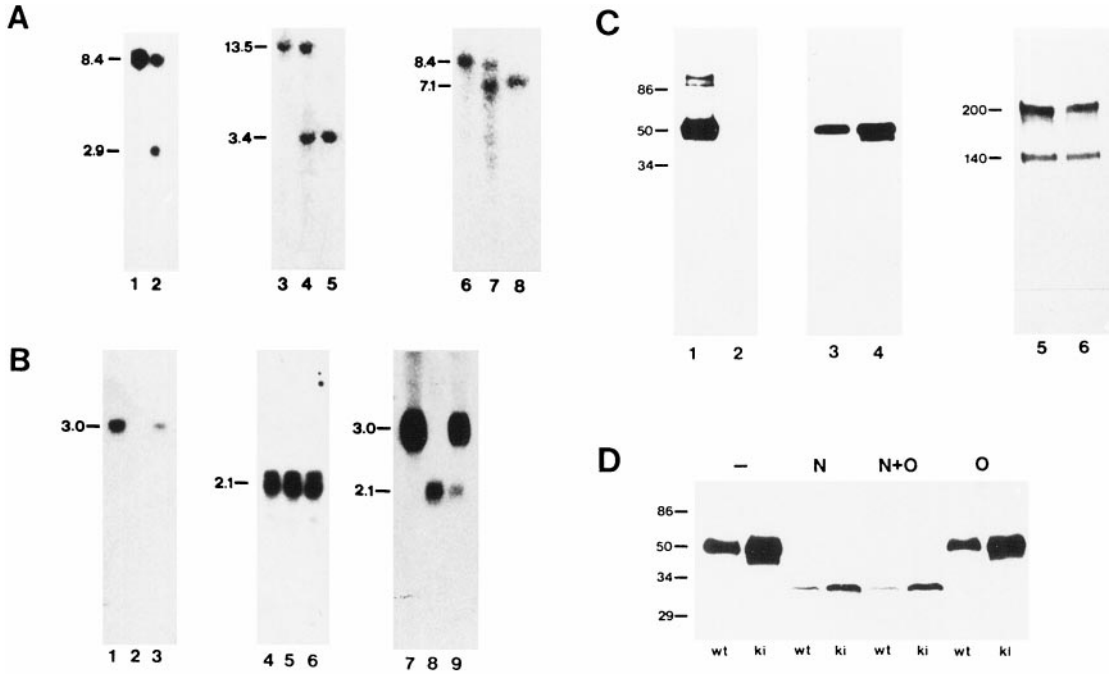

Figure 2. Southern blot analysis of $\beta2/\beta1^{+/+}$ and $\beta2/\beta1^{+/ki}$ targeted embryonic stem cells, and Southern, Northern, and Western blot analysis of $\beta2/\beta1^{+/+}$, $\beta2/\beta1^{+/ki}$, and $\beta2/\beta1^{ki/ki}$ mice. *A*, Southern blot analysis. DNA from $\beta2/\beta1^{+/+}$ (*lane 1*) and $\beta2/\beta1^{+/ki}$ targeted embryonic stem cells (*lane 2*) and DNA from $\beta2/\beta1^{+/+}$ (*lanes 3* and *6*), $\beta2/\beta1^{+/ki}$ (*lanes 4* and *7*), and $\beta2/\beta1^{ki/ki}$ (*lanes 5* and *8*) mice digested with *Bam*HI (*lanes 1, 2, 6–8*) or *Eco*RI (*lanes 3–5*) was hybridized with probes 5′EXT (*lanes 1–5*) or 3′INT (*lanes 6–8*). The size of DNA fragments in kilobases is indicated at the *left margin*. *B*, Northern blot analysis. RNA from brains of $\beta2/\beta1^{+/+}$ (*lanes 1, 4*, and *7*), $\beta2/\beta1^{+/ki}$ (*lanes 3, 6*, and *9*), and $\beta2/\beta1^{ki/ki}$ (*lanes 2, 5*, and *8*) mice was hybridized with probe β2 (exon II to exon VII; *lanes 1–3*), probe β1 (*lanes 4–6*), or probe β2–5′UT specific for the 5′ untranslated region of the β2 mRNA also present in the β2/β1 *knock-in* fusion mRNA (*lanes 7–9*). The size of RNA fragments in kilobases is indicated at the left margin. *C*, Western blot analysis with 10 μg of protein per lane of detergent extracts from crude membrane fractions from brains of 5-week-old $\beta2/\beta1^{+/+}$ (*lanes 1, 3*, and *5*) and $\beta2/\beta1^{ki/ki}$ (*lanes 2, 4*, and *6*) mice using polyclonal antibodies against β2 (*lanes 1* and *2*), and monoclonal antibodies BSP/3 against β1 (*lanes 3* and *4*). Polyclonal antibodies against L1 were used to confirm equal loading of proteins (*lanes 5* and *6*). β2 and β1 are clearly detectable as broad bands at 47–53 and 43 kDa, respectively (*lanes 1, 3*, and *4*). No signal with polyclonal β2 antibodies is obtained in $\beta2/\beta1^{ki/ki}$ (*lane 2*), whereas an additional band of ~40 kDa is observed with monoclonal antibodies BSP/3 (*lane 4*). The molecular mass is indicated at the left margin. *D*, Western blot analysis of deglycosylated proteins. Ten micrograms of soluble fractions of detergent lysates of crude membrane fractions from retinae of 17-d-old $\beta2/\beta1^{+/+}$ (*wt*) and $\beta2/\beta1^{ki/ki}$ (*ki*) mice were incubated with *N*-glycosidase F (*N*), *O*-glycosidase (*O*), both enzymes (*N* + O), or without enzyme (−), subjected to SDS-gel electrophoresis, and reacted with monoclonal antibody BSP/3 after Western blotting. Molecular mass standards are indicated in kilodaltons at the left margin.

probe β2–5′UT. A signal corresponding to β2 mRNA of ~3.0 kb was detectable in wild-type and heterozygous mice, whereas no signal of this size was detectable with RNA from β2/β1 *knock-in* mice. However, an additional band at ~2.1 kb corresponding to the transcript of the *knock-in* β1 gene was detected in heterozygous and homozygous β2/β1 *knock-in* mice with an intensity corresponding to ~10–20% of wild-type β2 mRNA expression (Fig. 2*B*).

To confirm that the mutation generated a null allele for β2, proteins from membrane fractions of brains of 5-week-old wild-type and β2/β1 *knock-in* mice were subjected to immunoblot analysis. The β2 subunit of the Na,K-ATPase was detectable in 10 μg of protein from brains of wild-type mice using a polyclonal antibody to the mouse β2 subunit, whereas no signal could be detected in the same amount of protein from brains of β2/β1 *knock-in* mice (Fig. 2*C*). To determine the amount of β1 protein, 10 μg of protein from brains of 5-week-old wild-type and β2/β1 *knock-in* mice were subjected to Western blot analysis using monoclonal antibody BSP/3. The β1 subunit of the Na,K-ATPase was detectable with a molecular mass of ~43 kDa in wild-type mice and in higher amounts in β2/β1 *knock-in* mice. This increase in β1 expression in β2/β1 *knock-in* mice amounted to 20–30% of that found in wild-type animals. In addition, a band of ~40 kDa was observed by immunoblot analysis in β2/β1 *knock-in* mice (Fig. 2*C*).

To determine whether this additional band is caused by a different glycosylation pattern of the β1 subunit, the carbohydrate contribution to the molecular mass and the type of carbohydrate modification were analyzed. Proteins (10 μg) from membrane fractions of retinae from 17-d-old wild-type and β2/β1 *knock-in* mice were subjected to enzymatic deglycosylation. After PNGase F treatment, the molecular masses of all β1-immunoreactive proteins from retinae of wild-type and β2/β1 *knock-in* mice were reduced. The band at 43 kDa in wild-type and β2/β1 *knock-in* mice and the additional band at 40 kDa in β2/β1 *knock-in* mice shifted to a single band at ~33 kDa. No change in the molecular mass of BSP/3-immunoreactive proteins was observed after treatment with *O*-glycosidase (Fig. 2*D*).

Analysis of β2/β1 *knock-in* mice by immunohistochemistry

In retinae of 17-d-old and 4-month-old wild-type mice, the plexiform layers and the ganglion cell layer showed immunoreactivity for the β1 subunit (Fig. 3*a,e*), whereas strongest immunoreactivity for the β2 subunit was detected in association with the inner segments of photoreceptor cells (Fig. 3*b,f*). In retinae of 17-d-old and 4-month-old β2/β1 *knock-in* mice, immunoreactivity for the β1 subunit was detected not only in the plexiform layers and the ganglion cell layer but also in the inner segments of photorecep-

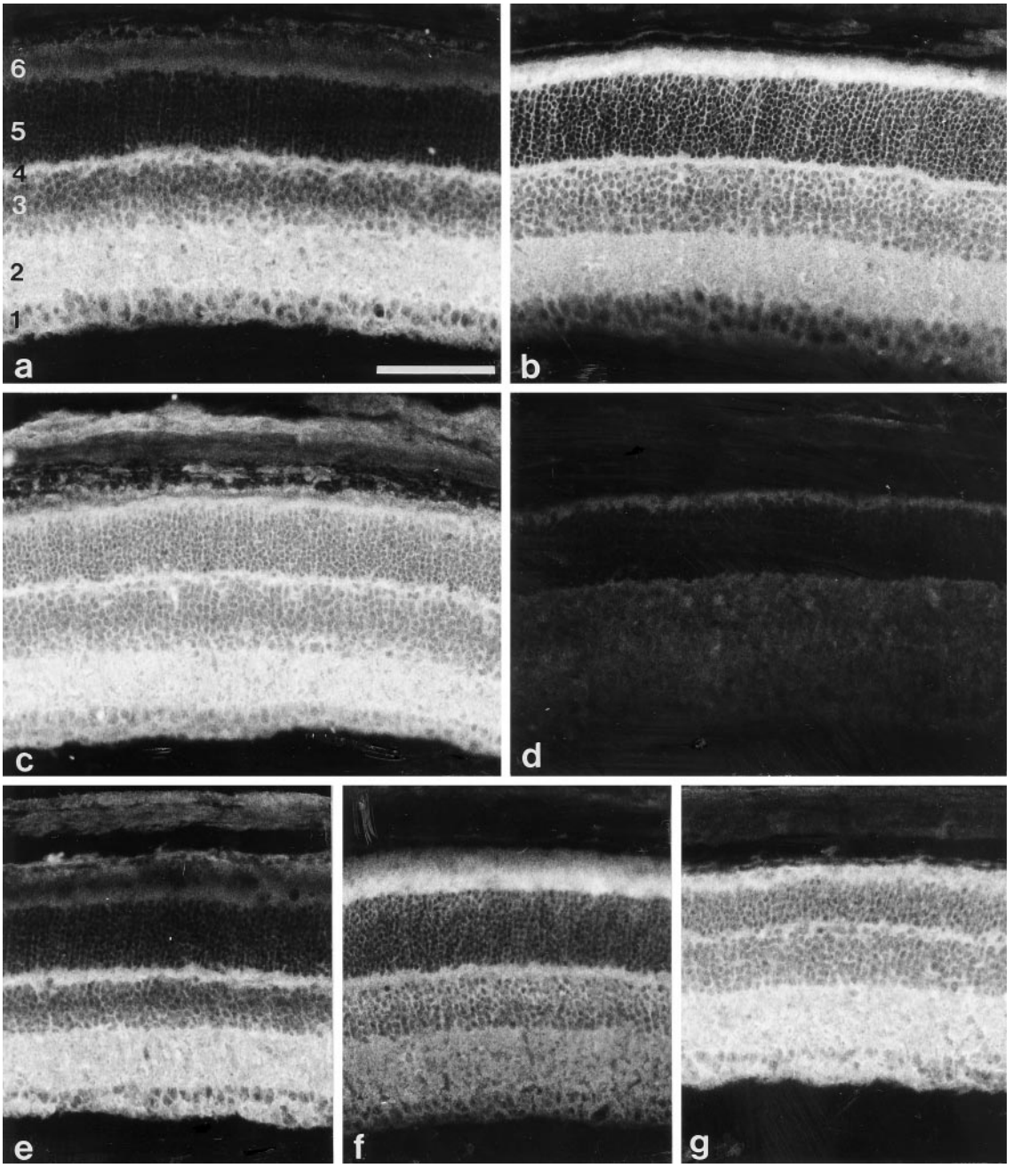

Figure 3. Immunohistological analysis of $\beta 2/\beta 1^{+/+}$ and $\beta 2/\beta 1^{ki/ki}$ mice. Immunohistological localization of $\beta 1$ (*a, c*) and $\beta 2$ (*b*) in sections of 17-d-old $\beta 2/\beta 1^{+/+}$ (*a, b*) or $\beta 2/\beta 1^{ki/ki}$ (*c*) retinae using monoclonal antibodies BSP/3 (*a, c*) and 426 (*b*) recognizing $\beta 1$ and $\beta 2$ isoforms, respectively. Note the intense $\beta 1$ immunoreactivity of inner segments of photoreceptor cells of $\beta 2/\beta 1^{ki/ki}$ mice. No $\beta 2$ immunoreactivity is detectable on sections from $\beta 2/\beta 1^{ki/ki}$ mice incubated with monoclonal antibody 426 (*d*). The immunohistological localization of $\beta 1$ (*e, g*) and $\beta 2$ (*f*) in sections of 4-month-old $\beta 2/\beta 1^{+/+}$ (*e, f*) or $\beta 2/\beta 1^{ki/ki}$ (*g*) retinae using monoclonal antibody BSP/3 (*e, g*) or 426 (*f*). Note the expression of $\beta 1$ by photoreceptor cells of $\beta 2/\beta 1^{ki/ki}$ mice (*g*). *1*, Ganglion cell layer and nerve fiber layer; *2*, inner plexiform layer; *3*, inner nuclear layer; *4*, outer plexiform layer; *5*, outer nuclear layer; *6*, inner and outer segments of photoreceptor cells. Scale bar (shown in *a* for *a–g*): 100 μm.

tor cells (Fig. 3*c,g*). Immunoreactivity for the $\beta 2$ subunit was not observed in retinae of $\beta 2/\beta 1$ *knock-in* mice (Fig. 3*d*).

Morphological analysis of retinae of $\beta 2/\beta 1$ *knock-in* mice

At the light microscopic level, the overall morphology of the brain was similar between wild-type and $\beta 2/\beta 1$ *knock-in* littermates at the ages of 17 d, 4 months, and 9 months. In contrast to $\beta 2$-deficient mice, neither enlarged ventricles nor swollen astrocytic end feet were observed in the brain stem, thalamus, or spinal cord of $\beta 2/\beta 1$ *knock-in* mice (data not shown). Furthermore, the cytoarchitecture of the cerebellar cortex of $\beta 2/\beta 1$ *knock-in* mice appeared normal and the thickness of different cortical layers was similar to that of wild-type littermates (data not shown).

Semithin sections through central regions of the retinae of 17-d-old, 4-month-old, and 9-month-old wild-type and $\beta 2/\beta 1$ *knock-in* littermates revealed a progressing degeneration of pho-

toreceptor cells in the mutants. In retinae of 17-d-old β2/β1 *knock-in* mice, the thickness of the outer nuclear layer appeared similar to that of age-matched wild-type animals (Fig. 4*a,b*), whereas the thickness of the outer nuclear layer in β2 *knock-out* mice was reduced in thickness (Fig. 4*c*). In retinae of 4-month-old β2/β1 *knock-in* mice, a reduction in the thickness of the outer nuclear layer was observed when compared with wild-type animals (Fig. 4*d,e*). In retinae of 9-month-old β2/β1 *knock-in* mice, the outer nuclear layer was either absent (data not shown) or reduced to a few rows or a single row of photoreceptor cells (Fig. 4*g*). In the mutant, the lengths of inner and outer segments of photoreceptor cells were significantly reduced when compared with wild-type littermates (Fig. 4, compare *f*, *g*). Analysis of retinae from wild-type and β2/β1 *knock-in* mice by electron microscopy confirmed a progressing degeneration of photoreceptor cells in retinae of 17-d-old, 4-month-old, and 9-month-old mutant mice (for 4-month-old wild-type and mutant animals, see Fig. 5, *a* and *b*, respectively).

Detection of apoptotic cell death in the retina of β2/β1 *knock-in* mice

Degeneration of photoreceptor cells in central regions of the retinae of 17-d-old, 4-month-old, and 9-month-old wild-type and β2/β1 *knock-in* mice was visualized using a modified TUNEL method (Molthagen et al., 1996). In retinae of 17-d-old wild-type mice, only a few degenerating cells were visible in the outer nuclear layer (Fig. 6*a*). In comparison, a significantly increased number of apoptotic photoreceptor cells was detectable in retinae of 17-d-old β2/β1 *knock-in* mice (Fig. 6*b*), but it was still below the number of apoptotic cells observed in 17-d-old retinae of β2 *knock-out* mice (Fig. 6*c*). In retinae of 4-month-old (Fig. 7*a*) or 9-month-old wild-type mice, hardly any degenerating cells were visible, whereas in age-matched β2/β1 *knock-in* mice (Fig. 7*b*) numerous apoptotic photoreceptor cells were detectable.

Quantitative determination of the density of TUNEL-labeled cells revealed that at postnatal day 17 the number of apoptotic photoreceptor cells was increased in mutant β2/β1 *knock-in* mice (132.3 ± 24.0 TUNEL-labeled cells per mm^2; mean ± SEM) when compared with wild-type mice (33.8 ± 3.2 TUNEL-labeled cells per mm^2; $p < 0.0001$) (Fig. 8). In 4-month-old wild-type mice, the number of degenerating photoreceptor cells was reduced to only very few cells (7.0 ± 1.0 TUNEL-labeled cells per mm^2), whereas in age-matched β2/β1 *knock-in* mice the number of apoptotic cells increased significantly (175.2 ± 7.2 TUNEL-labeled cells per mm^2; $p < 0.0001$) (Fig. 8). The highest density of degenerating photoreceptor cells was found in the outer nuclear layer of 9-month-old β2/β1 *knock-in* mice (265.3 ± 28.2 TUNEL-labeled cells per mm^2). Retinae of age-matched wild-type mice contained 5.3 ± 0.8 apoptotic cells per mm^2 ($p < 0.0001$) (Fig. 8).

DISCUSSION

We have generated *knock-in* mice expressing the β1 isoform instead of the β2 isoform of the Na,K-ATPase via homologous recombination in embryonic stem cells. The cDNA sequence coding for the β1 subunit was inserted in frame into the first exon of the β2 gene, thereby abolishing β2 gene expression. The deduced fusion protein contains 18 residues of the N-terminal part of β2, followed by residues 14 to 304 of β1. Southern blot analysis with 5′ external and 3′ internal β2 probes showed the hybridization pattern expected after homologous recombination. The absence of β2 gene expression in the mutant was confirmed by Northern blot, Western blot, and immunohistochemical analysis.

Northern blot analysis revealed transcription of the inserted β1 cDNA in the *knock-in* mice but to a lower extent than β2 gene transcription in the wild-type, possibly because of reduced stability of the primary transcript. This β1 transcript amounted to only 10–20% of the β2 transcript in the wild-type mice. The level of expression of the introduced β1 cDNA was below detection for *in situ* hybridization analysis using digoxigenin-labeled β1-specific cRNA probes (our unpublished observations). By Western blot analysis, expression of β1 subunit protein from the *knock-in* cDNA in mutant mice was revealed and amounted in retina extracts to 20–30% more β1 in comparison with β1 expression in the wild-type mice. Detection of an additional smaller band in tissue extracts from mutant mice recognized by an antibody against the β1 subunit suggested an additional β1 isoform caused by altered glycosylation. After deglycosylation with PNGase F, all β1-immunoreactive bands shifted to one single band at ~33 kDa, indicating a different glycosylation pattern of the *knock-in*-derived β1 protein compared with the endogenous β1 subunit in at least some cell types. Expression of the *knock-in* β1 subunit by cells normally expressing the β2 subunit may explain this change in the glycosylation of the β1 subunit. The β-isoforms of the Na,K-ATPase are only *N*-glycosylated with three or nine glycosylation sites predicted from the β1 and β2 sequences, respectively (Antonicek et al., 1987; Fahrig et al., 1990). As described previously, *O*-linked glycosylation was not observed for any of the BSP/3-positive components detected in either genotype.

Expression of the β1 subunit from the *knock-in* gene was further confirmed by immunohistochemical analysis, which revealed expression of the β1 subunit instead of β2 by photoreceptor cells in the retina of β2/β1 *knock-in* mice. The different reactivities of the antibodies recognizing either β2 or β1 subunits, however, did not permit a quantitative comparison between endogenous β2 and *knock-in* β1 protein expression levels. The use of antibodies raised against the first 18 residues of the β2 subunit and also contained in the β2/β1 *knock-in* protein may clarify this problem, under the assumption that these are not cleaved by proteases.

In contrast to β2-deficient mice, β2/β1 *knock-in* mice have a normal life span. Thus, expression of the β1 subunit in place of β2 abolishes the lethal phenotype reported for β2-deficient mice (Magyar et al., 1994). Deficits in motor coordination, tremors, or paralysis of extremities were not observed. Moreover, the abnormal histological phenotype in some brain regions of β2-deficient mice (Magyar et al., 1994) was not observed, and the general morphology of ventricles and other brain structures in β2/β1 *knock-in* mice appeared normal. Spongiform encephalopathy characterized by intracellular vacuoles in the brain tissue of β2-deficient mice (Magyar et al., 1994) was not observed in β2/β1 *knock-in* mice. At least to some extent, the β1 subunit of the Na,K-ATPase can functionally substitute for the β2 subunit, and the absence of an abnormal histological phenotype as described for some brain regions of β2-deficient mice implies a functional compensation for the absence of the β2 subunit by the *knock-in* β1 isoform. Our results support the interpretation that the basis of the phenotype of β2-deficient mice is caused by altered Na,K-ATPase pump activity (Magyar et al., 1994). It was shown that all six possible isozymes between α1, α2, α3 and β1 and β2 can be formed *in vitro*, supporting the assumption that different isozymes exist *in vivo* (Lemas et al., 1994; Schmalzing et al., 1997). Al-

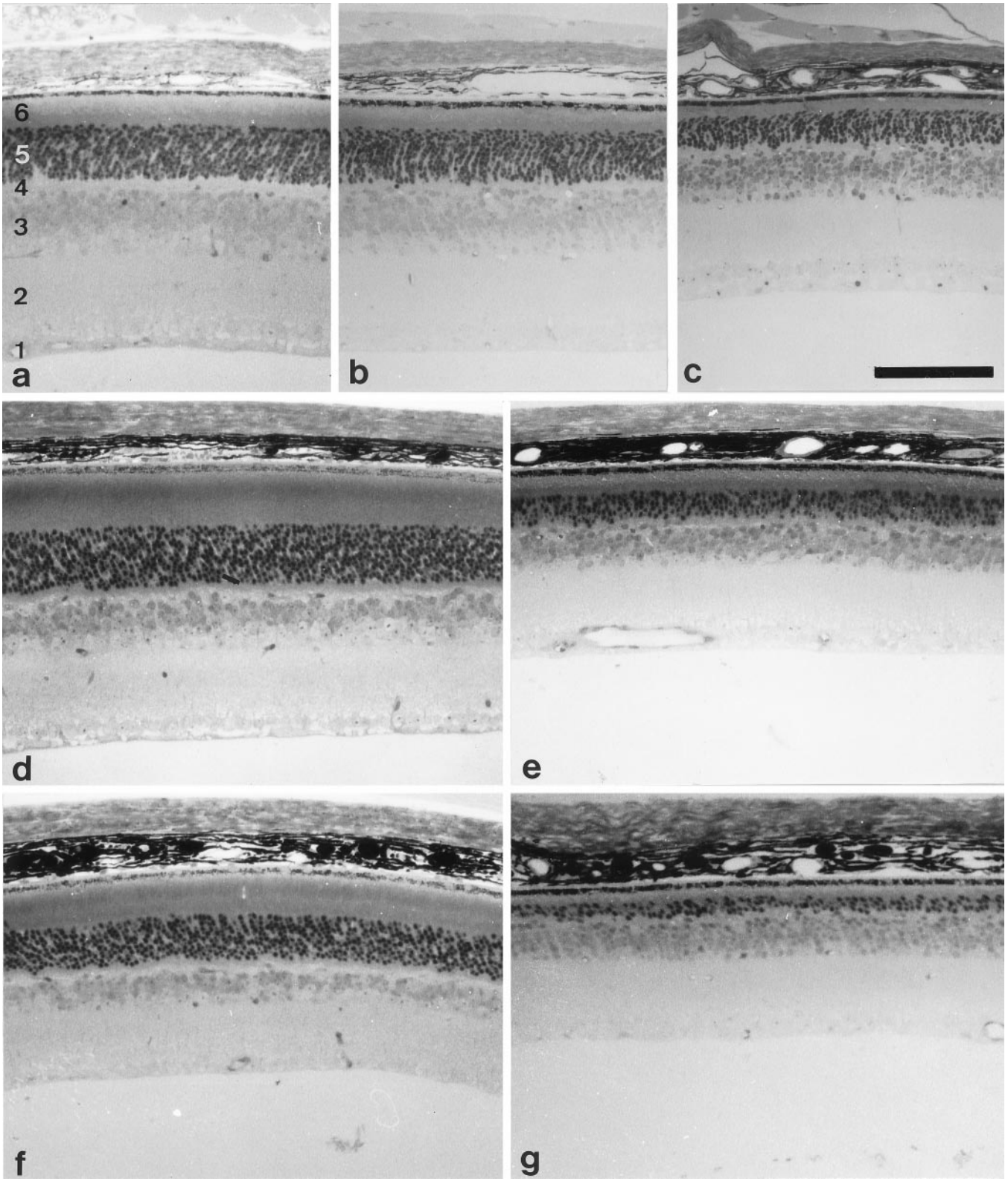

Figure 4. Light microscopic analysis of retinae of $\beta 2/\beta 1^{+/+}$ and $\beta 2/\beta 1^{ki/ki}$ mice. Semithin sections through retinae of 17-d-old (*a–c*), 4-month-old (*d, e*), and 9-month-old (*f, g*) $\beta 2/\beta 1^{+/+}$ (*a, d, f*), $\beta 2^{-/-}$ (*c*), and $\beta 2/\beta 1^{ki/ki}$ (*b, e, g*) mice. Note that the thickness of the outer nuclear layer and the length of the inner and outer segments of photoreceptor cells is significantly reduced in 17-d-old $\beta 2^{-/-}$ (*c*) and 4-month-old $\beta 2/\beta 1^{ki/ki}$ mice (*e*), and dramatically reduced in 9-month-old $\beta 2/\beta 1^{ki/ki}$ mutants when compared with age-matched wild-types (*a, d, f*). *1*, Ganglion cell layer and nerve fiber layer; *2*, inner plexiform layer; *3*, inner nuclear layer; *4*, outer plexiform layer; *5*, outer nuclear layer; *6*, inner and outer segments of photoreceptor cells. Scale bar (shown in *c* for *a–g*): 100 μm.

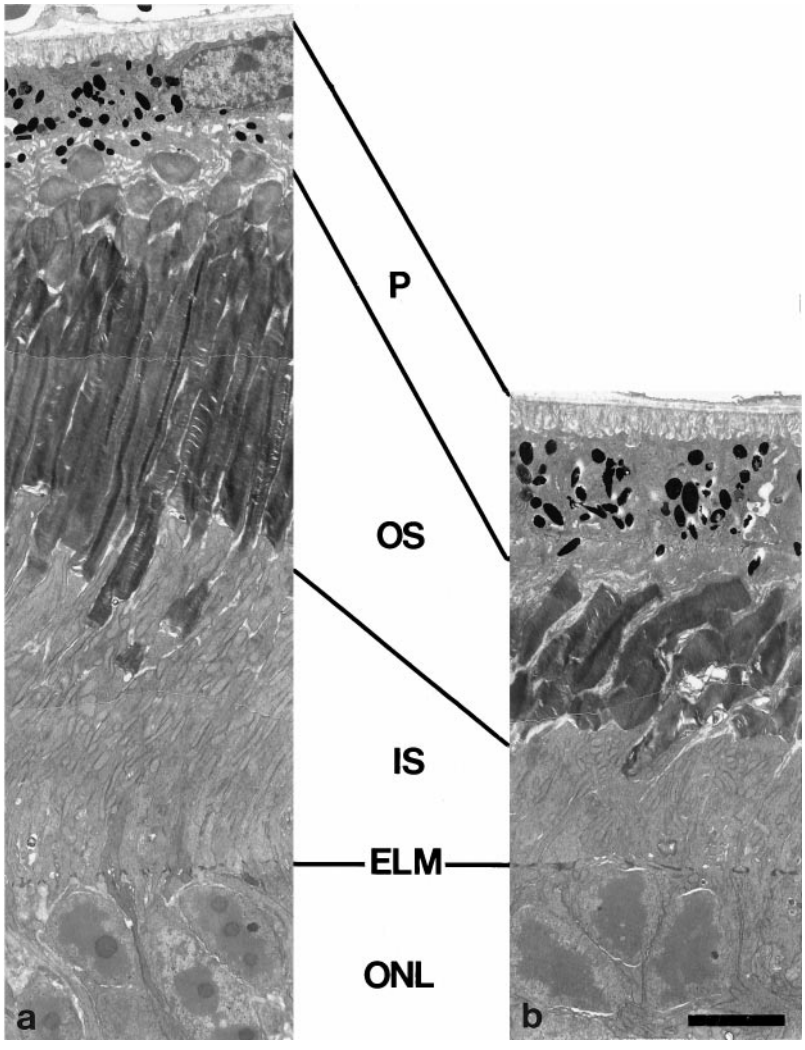

Figure 5. Electron microscopic analysis of photoreceptor cells of $\beta2/\beta1^{+/+}$ and $\beta2/\beta1^{ki/ki}$ mice. Ultrathin sections through retinae of 4-month-old $\beta2/\beta1^{+/+}$ (*a*) and $\beta2/\beta1^{ki/ki}$ (*b*) mice. Note that the length of inner and outer segments of photoreceptor cells in $\beta2/\beta1^{ki/ki}$ animals (*b*) is significantly reduced when compared with $\beta2/\beta1^{+/+}$ littermates (*a*). *ELM*, External limiting membrane; *IS*, inner segments; *ONL*, outer nuclear layer; *OS*, outer segments; *P*, pigment epithelium. Scale bar (shown in *b* for *a*, *b*): 5 μm.

though different kinetic properties of functional α–β-isozymes of the Na,K-ATPase have been described (Blanco et al., 1995a,b), sufficient ionic homeostasis seems to be achieved in many cells in which expression of the β2 subunit is substituted by β1 expression, resulting in an apparently normal phenotype in the *knock-in* animals regarding the spongiform encephalopathy and enlarged ventricles detected in β2-deficient mice. The complex temporal and spatial regulation of expression of the different α and β subunits by distinct cell types thus may provide a system for the optimal regulation of Na,K-ATPase pump activity.

In support of this view, we detected in the *knock-in* mutant animals a higher level of photoreceptor cell death than in wild-type animals. In β2-deficient mice, apoptotic death of photoreceptor cells in the retina was observed during the last days of the mutant's life (Molthagen et al., 1996), whereas in wild-type animals, apoptotic cell death in the retina occurs predominantly until the second postnatal week and after this time only sporadic cell loss is observed (Chang et al., 1993; Portera-Cailliau et al., 1994). Using the TUNEL method to analyze apoptotic cell death in retinae of β2/β1 *knock-in* mice, we observed a progressive degeneration of photoreceptor cells, although it was less than in β2-deficient mice [this study and Molthagen et al. (1996)]. Thus, apoptotic cell death of photoreceptor cells in the retina was delayed considerably in the *knock-in* mice compared with β2-deficient mice. The progressive loss of photoreceptor cells in the retina of β2/β1 *knock-in* mice leads to a reduction in the thickness of the outer nuclear layer. Furthermore, inner and outer segments of photoreceptor cells in retinae of 9-month-old β2/β1 *knock-in* mice were hardly detectable. The progressive cell death of photoreceptor cells in β2/β1 *knock-in* mice may be indicative of a suboptimal or insufficient Na,K-ATPase activity needed for the highly active photoreceptor cells. The α–β1-isozyme of the Na,K-ATPase may possess kinetic properties different from those of the α–β2 isozyme causing the degeneration of these particular cells. Alternatively, photoreceptor cells may depend on a particularly high Na,K-ATPase activity for which the level of β1 subunit expression may be insufficient in the β2/β1 *knock-in* mice. On the other hand, the phenotype of the *knock-in* mutant may be explained by the absence of the adhesive properties of the β2 subunit. Because the RNA expression level from the *knock-in* gene was lower than from the β2 gene in wild-type animals and the amount of protein cannot be compared directly, we cannot rule out either possibility. Using the *knock-in* mice to dissect the two functions of the AMOG/β2 molecule as a pump, on the one hand, and as an adhesion molecule, on the other hand, was thus possible only for cells in which sufficient ionic homeostasis was reached.

The selective loss of photoreceptor cells in β2/β1 *knock-in* mice resembles the human disease retinitis pigmentosa (RP). In photoreceptor-specific forms of human RP, night blindness and

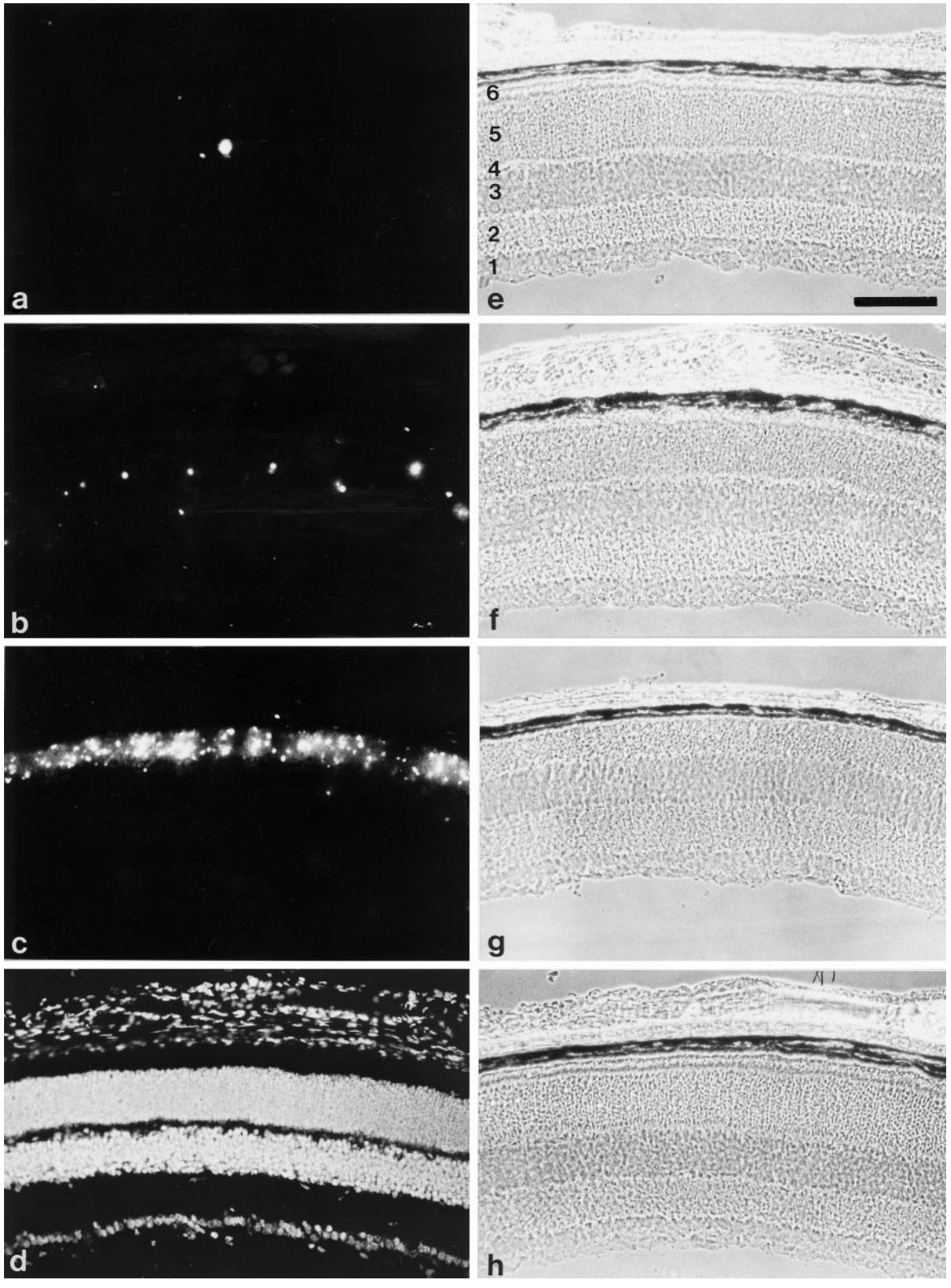

Figure 6. Apoptotic cell death of photoreceptor cells in 17-d-old $\beta 2/\beta 1^{+/+}$, $\beta 2/\beta 1^{ki/ki}$, and $\beta 2^{-/-}$ mice. Visualization of apoptotic cell death in the retina of 17-d-old $\beta 2/\beta 1^{+/+}$ (*a*), $\beta 2/\beta 1^{ki/ki}$ (*b*), and $\beta 2^{-/-}$ (*c*) mice using the TUNEL method. In the retina of 17-d-old $\beta 2/\beta 1^{+/+}$ animals, only a few degenerating photoreceptor cells are detectable (*a*). In contrast, in retinae of 17-d-old $\beta 2/\beta 1^{ki/ki}$ mice (*b*), apoptotic cell death is increased when compared with wild-type mice. In comparison, massive apoptotic cell death is visible in the outer nuclear layer of 17-d-old $\beta 2$-deficient mice (*c*) (also see Molthagen et al., 1996). As a positive control, sections were incubated with DNaseI before the TUNEL method was applied, and all retinal cells are labeled (*d*). *e–h* represent the phase-contrast photomicrographs of *a–d*, respectively. *1*, Ganglion cell layer and nerve fiber layer; *2*, inner plexiform layer; *3*, inner nuclear layer; *4*, outer plexiform layer; *5*, outer nuclear layer; *6*, inner and outer segments of photoreceptor cells. Scale bar (shown in *e* for *a–h*): 100 μm.

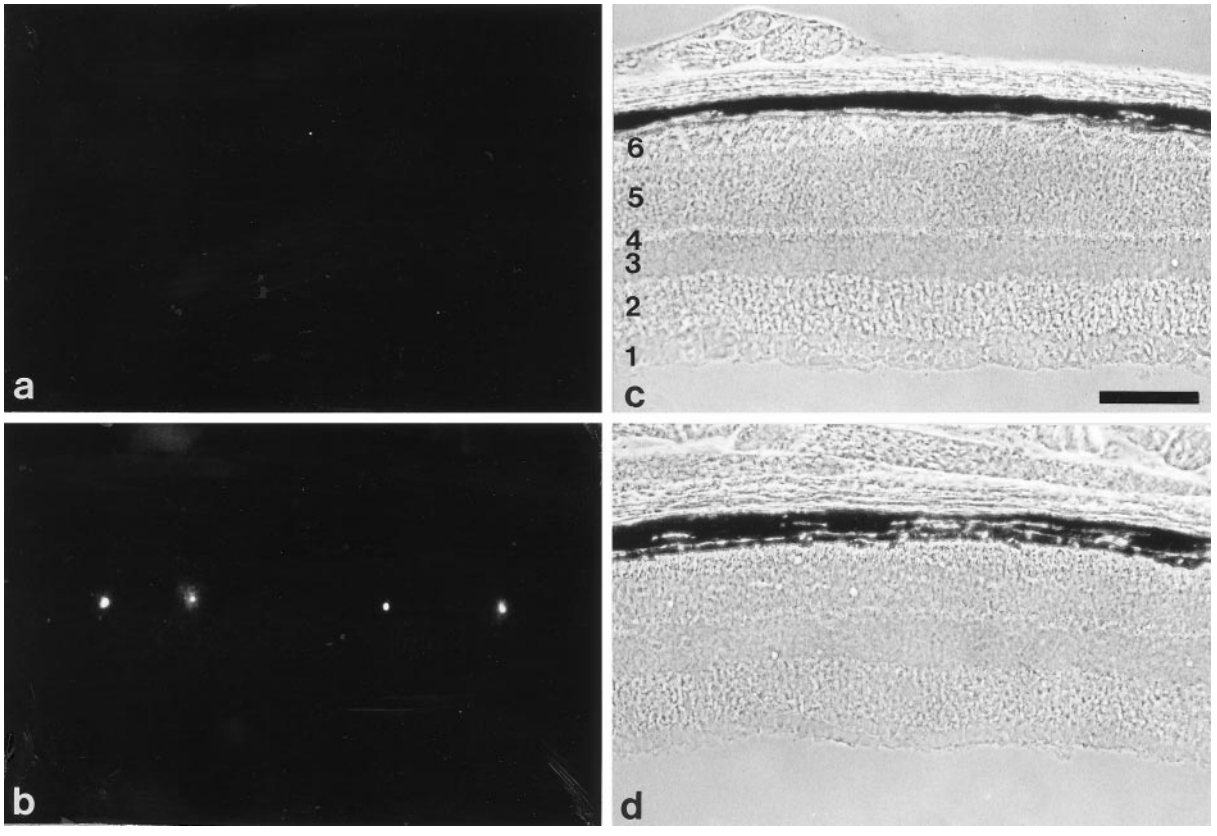

Figure 7. Apoptotic cell death of photoreceptor cells in 4-month-old $\beta2/\beta1^{+/+}$ and $\beta2/\beta1^{ki/ki}$ mice. Visualization of apoptotic cell death in the retina of 4-month-old $\beta2/\beta1^{+/+}$ (*a*) and $\beta2/\beta1^{ki/ki}$ (*b*) mice using the TUNEL method. In the retina of 4-month-old $\beta2/\beta1^{+/+}$ animals, apoptotic photoreceptor cells are virtually absent (*a*), whereas in retinae of 4-month-old $\beta2/\beta1^{ki/ki}$ mice (*b*), apoptotic cell death of photoreceptor cells is frequently observed. *c* and *d* represent the phase-contrast photomicrographs of *a* and *b*, respectively. *1*, Ganglion cell layer and nerve fiber layer; *2*, inner plexiform layer; *3*, inner nuclear layer; *4*, outer plexiform layer; *5*, outer nuclear layer; *6*, inner and outer segments of photoreceptor cells. Scale bar (shown in *c* for *a–d*): 100 μm.

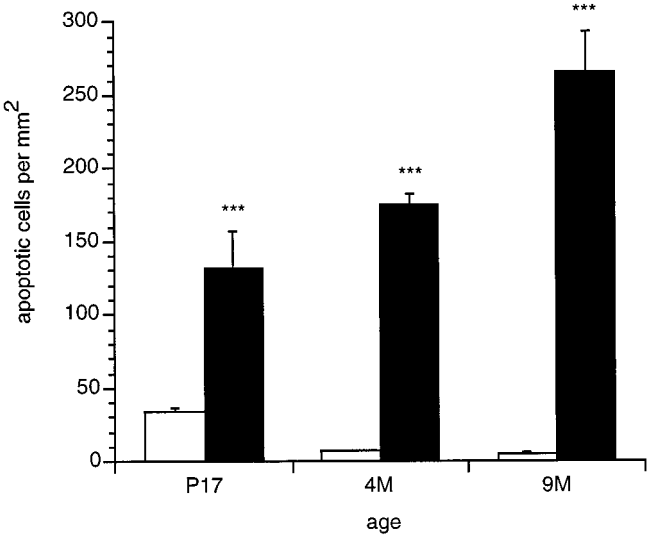

Figure 8. Density of TUNEL-labeled cells in the outer nuclear layer of $\beta2/\beta1^{+/+}$ (*open bars*) and $\beta2/\beta1^{ki/ki}$ (*filled bars*) mice at different ages. Animals were analyzed at postnatal day 17 (*P17*) and at 4 months (*4M*) and 9 months (*9M*) of age. Compared with wild-type mice, the density of apoptotic cells was significantly increased in the outer nuclear layer of $\beta2/\beta1^{ki/ki}$ mice at all ages analyzed (***$p < 0.0001$; according to Fischer's PLSD). Bars represent mean numbers of apoptotic photoreceptor cells/mm^2 ± SEM from at least three animals of each genotype and age.

loss of peripheral vision are the initial symptoms, reflecting degeneration of rod photoreceptors. Mutations in the genes for rhodopsin, peripherin, and cGMP phosphodiesterase have been identified in mouse models for some forms of RP (Dryja et al., 1990; Farrar et al., 1991; McLaughlin et al., 1993). It was shown that apoptotic cell death of photoreceptor cells occurs in these three mouse models (Chang et al., 1993; Portera-Cailliau et al., 1994). Photoreceptor cells undergo apoptosis not only during development for fine tuning the number of cells in the retina and their interconnections but also in maturity as a response to aberrant stimuli (Finlay, 1992). Internucleosomal DNA fragmentation that occurs during apoptotic cell death is thought to be mediated by a nuclear endonuclease that can be triggered by a rise in calcium concentration (Duke et al., 1983; Cohen and Duke, 1984; McConkey et al., 1989, 1990; Schwartzmann and Cidlowski, 1993). This mechanism of apoptosis was discussed for the *retinal degeneration* mouse, in which an increase in intracellular cGMP concentration initiates among other events a rise in calcium concentration (Chang et al., 1993). The Na,K-ATPase can directly influence the intracellular calcium concentration via the Na,Ca exchanger. In the β2/β1 *knock-in* mice, a malfunction of the Na,K-ATPase may also lead to altered intracellular concentrations of ions other than potassium and/or sodium and therefore to a similar induction of nuclear endonuclease activity, with the consequence of cell death. Studies are under way to

investigate this possibility and to use the β2/β1 *knock-in* mice as a model for retinitis pigmentosa.

REFERENCES

Antonicek H, Schachner M (1988) The adhesion molecule on glia (AMOG) incorporated into lipid vesicles binds to subpopulations of neurons. J Neurosci 8:2961–2966.

Antonicek H, Persohn E, Schachner M (1987) Biochemical and functional characterization of a novel neuron-glia adhesion molecule that is involved in neuronal migration. J Cell Biol 104:1587–1595.

Arystarkhova E, Sweadner KJ (1997) Tissue-specific expression of the Na,K-ATPase β3 subunit. The presence of β3 in lung and liver addresses the problem of the missing subunit. J Biol Chem 272:22405–22408.

Bartsch U, Kirchhoff F, Schachner M (1989) Immunohistological localization of the adhesion molecules L1, N-CAM, and MAG in the developing and adult optic nerve of mice. J Comp Neurol 284:451–462.

Blanco G, DeTomaso AW, Koster J, Xie ZJ, Mercer RW (1994) The α-subunit of the Na,K-ATPase has catalytic activity independent of the β-subunit. J Biol Chem 269:23420–23425.

Blanco G, Koster JC, Sánchez G, Mercer RW (1995a) Kinetic properties of the α2β1 and α2β2 isozymes of the Na,K-ATPase. Biochemistry 34:319–325.

Blanco G, Sánchez G, Mercer RW (1995b) Comparison of the enzymatic properties of the Na,K-ATPase α3β1 and α3β2 isozymes. Biochemistry 34:9897–9903.

Chan SY, Evans MJ (1991) In situ freezing of embryonic stem cells in multiwell plates. Trends Genet 7:76.

Chang GQ, Hao Y, Wong F (1993) Apoptosis: final common pathway of photoreceptor death in rd, rds, and rhodopsin mutant mice. Neuron 11:595–605.

Cohen JJ, Duke RC (1984) Glucocorticoid activation of calcium dependent endonuclease in thymocyte nuclei leads to cell death. J Immunol 132:38–42.

Dryja TP, McGee TL, Reichel E, Hahn LB, Cowley GS, Yandell DW, Sandberg MA, Berson EL (1990) A point mutation of the rhodopsin gene in one form of retinitis pigmentosa. Nature 343:364–366.

Duke RC, Chervenak R, Cohen JJ (1983) Endogenous endonuclease induced DNA fragmentation: an early event in cell-mediated cytolysis. Proc Natl Acad Sci USA 80:6361–6365.

Emanuel JR, Garetz S, Stone L, Levenson R (1987) Differential expression of Na,K-ATPase α and β subunit mRNAs in rat tissues and cell lines. Proc Natl Acad Sci USA 84:9030–9034.

Fahrig T, Schmitz B, Weber D, Kücherer-Ehret A, Faissner A, Schachner M (1990) Two monoclonal antibodies recognizing carbohydrate epitopes on neural adhesion molecules interfere with cell interactions. Eur J Neurosci 2:153–161.

Farrar GJ, Kena P, Jordan SA, Kumar-Singh R, Humphries MM, Sharp EM, Sheils DM, Humphries P (1991) A three-base-pair deletion in the peripherin-RDS gene in one form of retinitis pigmentosa. Nature 354:478–480.

Feinberg AP, Vogelstein B (1983) A technique for radiolabeling DNA restriction endonuclease fragments to high specific activity. Anal Biochem 132:6–13.

Finlay BL (1992) Cell death and the creation of regional differences in neuronal numbers. J Neurobiol 23:1159–1171.

Gavrieli Y, Sherman Y, Ben-Sasson SA (1992) Identification of programmed cell death *in situ* via specific labeling of nuclear DNA fragmentation. J Cell Biol 119:493–501.

Geering K (1991) The functional role of the β subunit in the maturation and intracellular transport of Na,K-ATPase. FEBS Lett 285:189–193.

Geering K, Theulaz I, Verrey F, Häuptle MT, Rossier BC (1989) A role for the β subunit in the expression of functional Na,K-ATPase in *Xenopus* oocytes. Am J Physiol 257:851–858.

Geering K, Beggah A, Good P, Girardet S, Roy S, Schaer D, Jaunin P (1996) Oligomerization and maturation of Na,K-ATPase: functional interaction of the cytoplasmic NH_2 terminus of the β subunit with the α subunit. J Cell Biol 13:1193–1204.

Gloor S (1989) Cloning and nucleotide sequence of the mouse Na,K-ATPase β subunit. Nucleic Acids Res 17:10117.

Gloor S, Antonicek H, Sweadner KJ, Pagliusi S, Frank R, Moos M, Schachner M (1990) The adhesion molecule on glia (AMOG) is a homologue of the β subunit of the Na,K-ATPase. J Cell Biol 110:165–174.

Gorvel GP, Liabeuf D, Massey D, Liot C, Goridis C, Maroux S (1984) Na,K-ATPase recognition in mouse organs by a monoclonal antibody. Cell Tissue Res 238:252–261.

Hara Y, Urayama O, Kawakami K, Nojima H, Nagamune H, Kojima T, Ohta T, Nagano K, Nakao M (1987) Primary structures of two types of α subunit of rat brain Na,K-ATPase deduced from cDNA sequences. J Biochem (Tokyo) 102:43–58.

Herrera VL, Emanuel JR, Ruiz-Opazo N, Levenson R, Nadal-Ginard B (1987) Three differentially expressed Na,K-ATPase α subunit isoforms: structural and functional implications. J Cell Biol 105:1855–1865.

Holm J, Hillenbrand R, Steuber V, Bartsch U, Moos M, Lübbert H, Montag D, Schachner M (1996) Structural features of a close homolog of L1 (CHL1) in the mouse: a new member of the L1 family of neural recognition molecules. Eur J Neurosci 8:1613–1629.

Hooper M, Hardy K, Handsyde A, Hunter S, Monk M (1987) HPRT-deficient (Lesch-Nyhan) mouse embryos derived from germline colonization by cultured cells. Nature 326:292–295.

Horisberger JD, Jaunin P, Good PJ, Rossier BC, Geering K (1991) Coexpression of α1 with putative β3 subunits results in functional Na+/K+ pumps in Xenopus oocytes. Proc Natl Acad Sci USA 88:8397–8400.

Jaisser F, Horisberger JD, Rossier BC (1992) The β subunit modulates potassium activation of the Na+/K+ pump. Ann N Y Acad Sci 671:113–119.

Jørgensen PL, Andersen JP (1988) Structural basis for E1–E2 conformational transitions in Na,K-pump and Ca-pump proteins. J Membrane Biol 103:95–120.

Laemmli UK (1970) Cleavage of structural proteins during the assembly of the head of bacteriophage T4. Nature 227:680–685.

Lecuona E, Luquin S, Avila J, Garcia-Segura LM, Martin-Vasallo P (1996) Expression of the β1 and β2 (AMOG) subunits of the Na,K-ATPase in neural tissues: cellular and developmental distribution patterns. Brain Res Bull 40:167–174.

Lemas MV, Yu HY, Takeyasu K, Kone B, Fambrough DM (1994) Assembly of Na,K-ATPase alpha-subunit isoforms with Na,K-ATPase beta-subunit isoforms and H,K-ATPase beta-subunit. J Biol Chem 269:18651–18655.

Magyar JP, Bartsch U, Wang ZQ, Howells N, Aguzzi A, Wagner EF, Schachner M (1994) Degeneration of neural cells in the central nervous system of mice deficient in the gene for the adhesion molecule on glia, the β2 subunit of the murine Na,K-ATPase. J Cell Biol 127:835–845.

Malik N, Canfield VA, Beckers MC, Gros P, Levenson R (1996) Identification of the mammalian Na,K-ATPase β3 subunit. J Biol Chem 271:22754–22758.

Mansour Sl, Thomas KR, Capecchi MR (1988) Disruption of the proto-oncogene int-2 in mouse embryo-derived stem cells: a general strategy for targeting mutations to non-selectable genes. Nature 336:348–352.

McConkey DJ, Nicotera P, Hartzell P, Bellomo G, Wyllie AH, Orrenius S (1989) Glucocorticoids activate a suicide process in thymocytes through an elevation of cytosolic Ca^{2+} concentration. Arch Biochem Biophys 269:365–370.

McConkey DJ, Chow SC, Orrenius S, Jondal M (1990) NK cell-induced cytotoxicity is dependent on a Ca^{2+} increase in the target. FASEB J 4:2661–2664.

McDonough AA, Geering K, Farley RA (1990) The sodium pump needs its β subunit. FASEB J 4:1598–1605.

McLaughlin ME, Sandberg MA, Berson EL, Dryja T (1993) Recessive mutations in the gene encoding the β subunit of rod phosphodiesterase in patients with retinitis pigmentosa. Nature Genet 4:130–134.

Mercer RW, Schneider JW, Savitz A, Emanuel J, Benz EJ, Levenson R (1986) Rat brain Na,K-ATPase beta-chain gene: primary structure, tissue-specific expression, and amplification in ouabain-resistant HeLa+ cells. Mol Cell Biol 6:3884–3890.

Molthagen M, Schachner M, Bartsch U (1996) Apoptotic cell death of photoreceptor cells in mice deficient for the adhesion molecule on glia (AMOG, the β2 subunit of the Na,K-ATPase). J Neurocytol 25:243–255.

Montag D, Giese KP, Bartsch U, Martini R, Lang Y, Blüthmann H, Karthigasan J, Kirschner DA, Wintergerst ES, Nave KA, Zielasek J, Toyka KV, Lipp HP, Schachner M (1994) Mice deficient for the myelin-associated glycoprotein show subtle abnormalities in myelin. Neuron 13:229–246.

Müller-Husman G, Gloor S, Schachner M (1993) Functional character-

ization of β isoforms of murine Na,K-ATPase. J Biol Chem 268:26260–26267.
Munzer JS, Daly SI, Jewell-Motz EA, Lingrel JB, Blostein R (1994) Tissue- and isoform-specific kinetic behaviour of the Na,K-ATPase. J Biol Chem 269:16668–16676.
Orlowski J, Lingrel JB (1988) Tissue-specific and developmental regulation of rat Na,K-ATPase catalytic α isoform and β subunit mRNAs. J Biol Chem 21:10436–10442.
Pagliusi SR, Schachner M, Seeburg PH, Shivers BD (1990) The adhesion molecule on glia (AMOG) is widely expressed by astrocytes in developing and adult mouse brain. Eur J Neurosci 2:471–480.
Peng L, Martin-Vasallo P, Sweadner KJ (1997) Isoforms of Na,K-ATPase α and β subunits in the rat cerebellum and in granule cell cultures. J Neurosci 17:3488–3502.
Portera-Cailliau C, Sung CH, Nathans J, Adler R (1994) Apoptotic photoreceptor cell death in mouse models of retinitis pigmentosa. Proc Natl Acad Sci USA 91:974–978.
Ramirez-Solis R, Rivera-Perez J, Wallace JD, Wims M, Zheng H, Bradley A (1992) Genomic DNA microextraction: a method to screen numerous samples. Anal Biochem 201:331–335.
Rathjen FG, Schachner M (1984) Immunocytological and biochemical characterization of a new neuronal cell surface component (L1 antigen) which is involved in cell adhesion. EMBO J 3:1–10.
Schmalzing G, Gloor S, Omay H, Kröner S, Appelhans H, Schwarz W (1991) Up-regulation of sodium pump activity in *Xenopus laevis* oocytes by expression of heterologous β1 subunits of the sodium pump. Biochem J 279:329–336.
Schmalzing G, Kröner S, Schachner M, Gloor S (1992) The adhesion molecule on glia (AMOG/β2) and α1 subunits assemble to functional sodium pumps in *Xenopus* oocytes. J Biol Chem 267:20212–20216.
Schmalzing G, Ruhl K, Gloor S (1997) Isoform-specific interactions of Na,K-ATPase subunits are mediated via extracellular domains and carbohydrates. Proc Natl Acad Sci USA 94:1136–1141.
Schwartzmann RA, Cidlowski JA (1993) Apoptosis: the biochemistry and molecular biology of programmed cell death. Endocr Rev 14:133–151.
Shull GE, Greeb J, Lingrel JB (1986) Molecular cloning of three distinct forms of the Na,K-ATPase α subunit from rat brain. Biochemistry 25:8125–8132.
Skou JC (1990) The energy coupled exchange of Na^+ for K^+ across the cell membrane. The Na,K-pump. FEBS Lett 268:314–324.
Soriano P, Montgomery C, Geske R, Bradley A (1991) Targeted disruption of the c-src proto-oncogene leads to osteopetrosis in mice. Cell 64:693–702.
Therien AG, Nestor NB, Ball WJ, Blostein R (1996) Tissue-specific versus isoform-specific differences in cation activation kinetics of the Na,K-ATPase. J Biol Chem 271:7104–7112.
Towbin H, Staehelin T, Gordon J (1979) Electrophoretic transfer of proteins from polyacrylamide gels to nitrocellulose sheets: procedure and some applications. Proc Natl Acad Sci USA 76:4350–4354.
Wintergerst ES, Fuss B, Bartsch U (1993) Localization of janusin mRNA in the central nervous system of the developing and adult mouse. Eur J Neurosci 5:299–310.